

Spatial and Kinetic Separation of Eley-Rideal Plus Primary Hot Atom and Secondary Hot Atom Mechanisms in H Atom Abstraction of Adsorbed D Atoms on Pt(111)

Jae-Young Kim and Jihwa Lee*

Division of Chemical Engineering, Seoul National University, Seoul 151-742, Korea

(Received 29 June 1998)

In the H(g)-on-D_{ad} abstraction reaction on a Pt(111) surface at 100 K, HD molecules are formed via direct Eley-Rideal and primary hot atom mechanisms as well as via a secondary hot atom mechanism with an equal yield but distinctively different kinetics and angular distributions peaked at $\sim 0^\circ$ and $\sim 45^\circ$ from the surface normal, respectively. However, the former two mechanisms are not distinguished in the present experiment. About 37% of adsorbed D atoms desorbed as D₂ formed via a secondary hot atom mechanism with a distribution also peaked at $\sim 45^\circ$. Results are discussed in terms of the reaction dynamics. [S0031-9007(99)08426-4]

PACS numbers: 79.20.Rf

Surface reactions of the gas-phase atoms of thermal energies with atomic and molecular adsorbates on metal and semiconductor surfaces have gained much attention in recent years because of the fundamental interest in the mechanism and dynamics of these reactions under nonequilibrium conditions in contrast to those of thermally activated reactions between adsorbed species (Langmuir-Hinshelwood (LH) mechanism). Abstraction of chemisorbed H(D) atoms by the gas-phase D(H) atoms is the simplest model reaction and therefore has been most extensively investigated theoretically as well as experimentally [1–10]. The results have been usually interpreted in terms of the Eley-Rideal (ER) mechanism in which an incident H(D) atom directly reacts upon making the first collision with the surface. For the reactions H(D) + D(H)/Cu(111) Rettner and Auerbach [7] have demonstrated that the reaction exothermicity of 2.3 eV is mostly carried away by the nascent HD molecules as translational, vibrational, and rotational energies with little dissipation to the surface, which suggests an impulsive nature of the reaction. However, the experimentally estimated abstraction cross section ($\sigma \sim 5 \text{ \AA}^2$ [7]) is larger by 1 order than that obtained by molecular dynamic calculations [8,9], which led to the suggestion that abstraction by hot atoms, which are trapped atoms but not accommodated to the surface, may be the dominant mechanism. Recently, in H-on-D_{ad} (D-on-H_{ad}) reaction D₂ (H₂) has been observed in addition to the major HD product on metal surfaces [11], which clearly demonstrates one type of hot atom-mediated reactions. Although the ER and hot atom reactions would exhibit different reaction dynamics in view of the different energies and lateral momenta of the incident and hot atoms, the two mechanisms have not been experimentally distinguished for hydrogen abstraction reactions so far by their product angular and/or energy distributions.

In this Letter, we have shown in the H-on-D_{ad} abstraction reaction on Pt(111) at 100 K that HD molecules are formed by direct ER plus primary hot atom reac-

tions as well as by secondary hot atom reactions with an equal yield but distinctively different angular distributions peaked at near the surface normal and at $\sim 45^\circ$, respectively. About 37% of adsorbed D atoms desorbed as D₂ formed by homonuclear secondary hot atom reaction with an angular distribution also peaked at $\sim 45^\circ$. The results are discussed in terms of the reaction dynamics.

The experiments have been performed in an ultrahigh vacuum system [12] equipped with an ion gun, Auger electron spectrometer, a hydrogen atom source, and two quadrupole mass spectrometers (QMS). The H(D) atom beam was produced in a narrow tungsten tube ($\phi_{\text{id}} = 1 \text{ mm}$) heated to $\sim 1900 \text{ K}$ by electron bombardment enclosed in a water-cooled radiation shield. The beam profile at the surface of the Pt(111) crystal, a disk of 9 mm diameter, $\sim 2 \text{ cm}$ from the tube tip was roughly measured to have a broad nonuniform distribution with a FWHM of $\sim 6 \text{ mm}$ in diameter, and therefore even at normal incidence the beam essentially floods the whole surface area. Two QMS's were employed for simultaneously measuring the total and angle-resolved product desorption rates: one mounted in the sample chamber and having no direct line of sight communication with the sample and the other housed in a differentially pumped can with two collimating apertures 1.6 and 3.3 cm from the surface (acceptance cone angle of $\sim 5^\circ$), respectively. For angle-resolved kinetic measurements the crystal was rotated with respect to the fixed atom source and QMS, whose axes make an angle of 45° at the sample surface, and therefore the incidence angle θ_i and desorption angle θ_f defined from the surface normal vary together according to the relation $\theta_f + \theta_i = 45^\circ$. For the product angular distribution (Fig. 3) the θ_f -dependent collection efficiency of the collimating apertures has been separately measured and corrected for; the angular distribution of O₂ desorbing at 150 K from the O₂-saturated Pt(111) surface in temperature-programmed desorption (TPD) turned out to be $\sim \cos^{0.5} \theta_f$, and its deviation from a $\cos \theta_f$ distribution expected for a molecular adsorbate whose adsorption

is nonactivated can be attributed to the θ_f -dependent collection efficiency. Before each run, the Pt(111) surface at 100 K was dosed with D atoms for 120 s, which was found to be enough to saturate the whole surface to have a coverage of $\theta_s = 1$ monolayer (ML) (1.5×10^{15} atoms/cm²).

In Fig. 1 we have shown the time-dependent QMS signals of HD and D₂ desorbing from the D-saturated Pt(111) at 100 K exposed to a beam of H atoms at $t = 0$, which were detected with the QMS in the sample chamber. Since a hydrogen molecule does not adsorb molecularly on Pt(111) at 100 K, the measured desorption rate $R(t)$ corresponds to the product formation rate. Taking into account the relative QMS sensitivities (HD : D₂ = 1.06 : 1), we have plotted the rates in a ML/s unit based on the D atom balance, i.e., $\int_0^\infty \{R_{HD}(t) + 2R_{D_2}(t)\} dt = \theta_D(0) = 1$ ML. Upon starting the reaction, the HD signal makes a step-like jump and then further increases slightly to the maximum which is followed by a monotonic decay, whereas the D₂ signal jumps to the maximum at $t = 0$ and then decays exponentially. The postreaction TPD measurement showed desorption of only H₂ but no other molecule, indicating that the initial surface D atoms were completely replaced by H atoms. H₂ was also produced by the abstraction reaction, but we could not get a quantitative data due to the large background. Integrating the rate curves, we find that $63 \pm 3\%$ of the initial surface D atoms desorb as HD and the rest $37 \pm 3\%$ as D₂. Although not shown here, the combined yield of HD and D₂ on a D atom basis and the product branching ratio were almost independent of θ_i , which implies that the whole surface area was

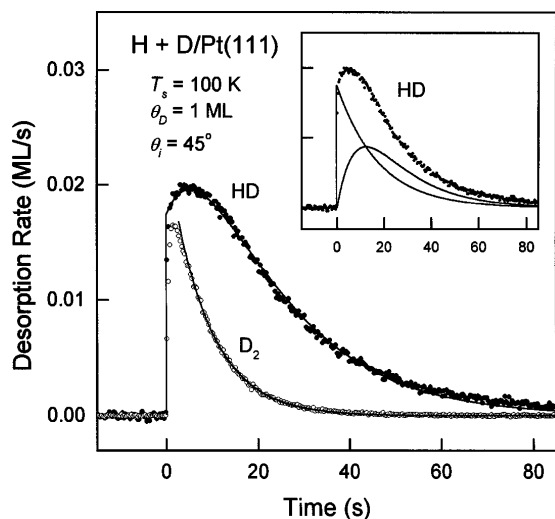


FIG. 1. Angle-integrated desorption rate curves of HD and D₂ formed in the reaction of the gas-phase H atom with the D atom adsorbed on Pt(111) at 100 K and saturation coverage. The solid curves represent the best-fitting functions of the form $f(t) = Ae^{-kt} + B(e^{-kt} - e^{-2kt})$ for HD, and $f(t) = Cd^{-2kt}$ for D₂ derived from a kinetic model. The inset shows kinetic separation of the HD signal into ER plus *p*-HA and *s*-HA reaction components (see the text).

sampled by the H atom beam at all incidence angles. The time constants associated with the exponentially decaying D₂ signal were found to be almost proportional to the inverse of $\cos \theta_i$. Thus, we conclude that the reaction rate is proportional to the H atom flux, and the flux effectively varies as close to $\cos \theta_i$ in the present experiment.

In Fig. 2 are shown the angle-resolved desorption rates of HD and D₂ measured at three different desorption angles of $\theta_f = 0^\circ$, 30° , and 60° , in which the incidence angles for the latter two ($\theta_i = \pm 15^\circ$) are actually the same. Two characteristic features of the data can be immediately noticed: (1) the rate curves of D₂ are qualitatively similar to the angle-integrated one in Fig. 1 at all desorption angles. The different decay rates are simply due to the θ_i -dependent H atom flux; (2) the shape of the rate curve of HD is strongly θ_f dependent. At $\theta_f = 0^\circ$, it shows a large initial jump followed by an exponential decay, whereas at $\theta_f = 60^\circ$ the signal is initially zero but increases to the maximum at a finite reaction time. At an intermediate angle of $\theta_f = 30^\circ$, a rate curve which is almost halfway between the other two is measured. It thus appears that HD molecules are formed via two different mechanisms with completely different reaction kinetics and product angular distributions. By time integrating the rate curves measured at various desorption angles, we have plotted the angular

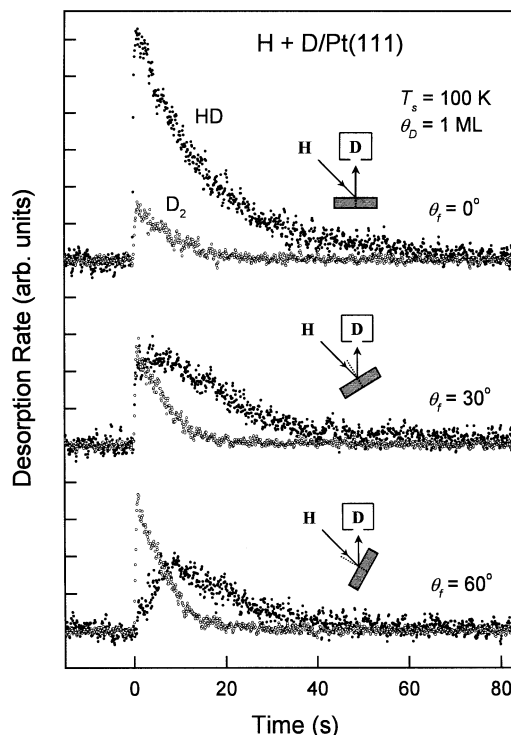
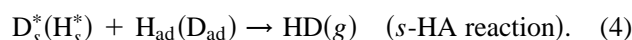
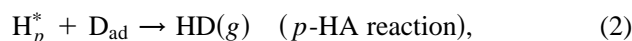
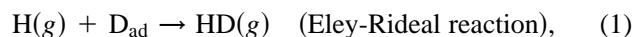


FIG. 2. Angle-resolved desorption rate curves of HD and D₂ formed in the reaction of the gas-phase H atom with the D atom adsorbed on Pt(111) at 100 K and saturation coverage, in which the geometrical configurations of the atom beam (H) and the detector (D), with respect to the sample, are schematically shown.

distributions of HD and D₂ (Fig. 3) after correcting for the θ_f -dependent collection efficiency of the collimators. HD shows two overlapping lobes with the main peak at $\theta_f \sim 10^\circ$ and the shoulder peak roughly at $\theta_f \sim 45^\circ$, which implies that the dynamics of HD formation involved in the two mechanisms mentioned above are quite different from each other resulting in different product angular distributions. On the other hand, the angular distribution of D₂ shows a broad distribution with a single peak at $\theta_f \sim 45^\circ$ and an appreciable intensity around the surface normal. The peak angle of $\sim 45^\circ$ is about the same as the shoulder peak of HD.

Now we consider possible reaction mechanisms via which HD and D₂ are formed. The H atom incident on a D-saturated Pt(111) surface simply reflects to the gas phase, directly abstracts a D_{ad} atom, or fails to react but is trapped in the surface potential well. Trapping may occur in collisions with Pt atom(s) with little energy transfer or in nonreactive energy-transfer collisions with adsorbed D(H) atoms. As a result, transient primary hot H_p^{*} atoms (*p*-HA) as well as secondary hot D_s^{*}(H_s^{*}) atoms (*s*-HA) will be generated, which may be energetic enough to abstract a surface D(H) atom during their hopping motions along the surface. Based on this picture, one can conceptually distinguish three different reaction mechanisms via which

HD and D₂ molecules are formed:



We have analyzed [12] the desorption rate curves by modeling the reaction kinetics based on these mechanisms under the constant total coverage condition $\theta_D + \theta_H = 1 \text{ ML}$ to get an approximate solution $\theta_D(t) \approx e^{-kt}$ for the D atom coverage and then the desorption rates in the form of $R_{\text{HD}}(t) = Ae^{-kt} + B(e^{-kt} - e^{-2kt})$ and $R_{\text{D}_2}(t) = Ce^{-2kt}$, where A , B , C , and k are constants. Although we have neglected relatively small isotope effects in the *s*-HA reactions in the analysis, the measured curves can be reasonably well fitted by these functions as shown by the solid curves in Fig. 1. The two terms in $R_{\text{HD}}(t)$ can be easily identified by noting that the rate of HD formation by the ER and *p*-HA reactions is proportional to θ_D while that by the heteronuclear *s*-HA reactions is proportional to $\theta_D \cdot \theta_H$, i.e., $R_{\text{HD}}(t) = A\theta_D + B\theta_D\theta_H = Ae^{-kt} + Be^{-kt}(1 - e^{-kt})$. This allows us to kinetically separate the HD signal into the ER plus *p*-HA and the *s*-HA reaction components (inset of Fig. 1). Thus, the rate curve of HD at $\theta_f = 0^\circ$ in Fig. 2 which shows a large initial jump followed by an exponential decay can be entirely attributed to the ER plus *p*-HA reactions, whereas the one at $\theta_f = 60^\circ$ to the heteronuclear *s*-HA reactions. We also find that $51 \pm 3\%$ of the total HD is formed via the *s*-HA mechanism and the rest via the ER and *p*-HA mechanisms. Similarly, we have separated the total angular distribution of HD into the ER plus *p*-HA and the *s*-HA reaction components as shown in Fig. 3. Although the error bars are relatively large, one can see that HD formed via the *s*-HA mechanism now shows an angular distribution peaked at about $\theta_f \sim 45^\circ$ with little intensity near $\theta_f \sim 0^\circ$, while that of the ER plus *p*-HA reaction component is sharply peaked near the surface normal. The latter distribution can be closely represented by $\cos^{12}(\theta_f - 3^\circ)$ as shown by the broken curve, which is very similar to a $\cos^9(\theta_f - 2^\circ)$ distribution that Rettner [4] measured for the H-on-D_{ad} reaction on Cu(111). However, the angular distribution he measured does not show a shoulder peak at a large desorption angle attributable to HD formed via *s*-HA mechanisms. The negligible contribution to HD formation by the *s*-HA mechanism on Cu(111) can be partly attributed to a smaller saturation coverage of the hydrogen atom on Cu(111) than that on Pt(111): $\sim 0.9 \times 10^{15}$ vs 1.5×10^{15} atoms/cm². Assuming conservation of the parallel momentum of the H(*g*) atom, Rettner [4] estimated a far greater HD desorption angle of $\sim 25^\circ$ than the observed peak shift of 2° , from which he suggested that the H(*g*) atom, which recovers most of the 2.4 eV heat of adsorption before striking the surface, deeply penetrates the

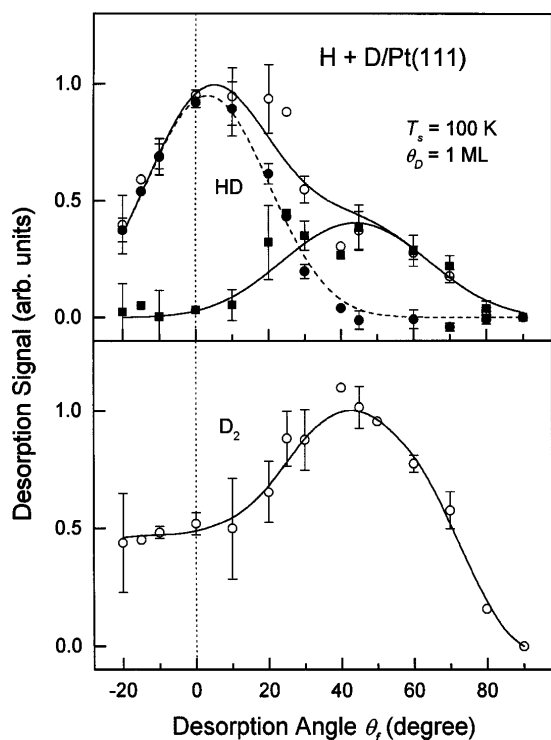


FIG. 3. Angular distributions of HD and D₂ (open symbols) plotted by integrating the rate curves in Fig. 2. The HD signal at each desorption angle was separated based on a kinetic model into the ER plus primary hot atom (●) and secondary hot atom (■) reaction components. The broken curve corresponds to a $\cos^{12}(\theta_f - 3^\circ)$ distribution. The solid curves are smoothly drawn as a mere guide.

surface potential to experience an appreciable corrugation, so that the memory of the small initial parallel momentum of the $H(g)$ atom is almost washed out to be only vaguely reflected in a small peak shift. A similar interpretation can be made for the angular distribution of HD formed via ER plus p -HA mechanisms on Pt(111). Thus, the peak shift of $\sim 3^\circ$ is attributed to the effect of the small initial parallel momentum of $H(g)$ which is partially carried away by the product molecules. According to the quasiclassical trajectory studies on the $H(D)$ -on- $D_{ad}(H_{ad})$ reaction on a corrugated Cu(111) by Caratzoulas *et al.* [9], most of the direct ER reactions occur at impact parameters of $b \leq 0.3 \text{ \AA}$ with a small cross section of $\sigma_{ER} \sim 0.28 \text{ \AA}^2$. If this is the case, the large cross section of $\sigma \sim 5 \text{ \AA}^2$ estimated experimentally by Rettner and Auerbach [7] is mostly due to HD formation via the p -HA mechanism. Although we could not separate the ER and p -HA reaction components from each other in the present experiment, we believe that the ER reaction component is also small on Pt(111). The p -HA's are expected to result mainly from trapping collisions of $H(g)$ atoms with Pt atoms with little energy transfer and parallel momentum gain, and therefore they will behave like $H(g)$ atoms as far as the abstraction reaction dynamics is concerned. This is probably the reason why we could not distinguish them in the angular distribution. However, some p -HA's may also result from corrugation-mediated trapping (selective adsorption) and direct nonreactive $H(g)$ -adatom collisions emerging with a sizable parallel momentum, but their abstraction products will only contribute to broadening of the angular distribution because of their azimuthally isotropic momenta. HD molecules once formed will be ejected out in near the surface normal directions by a repulsive but relatively weakly corrugated HD-surface potential.

On the other hand, energetic s -HA's will be mostly generated in direct nonreactive energy-transfer collisions of $H(g)$ atoms with adsorbed $D(H)$ atoms at impact parameters in the range of $0.3 < b < 0.74 \text{ \AA}$ (equilibrium bond length of H_2), in which the struck adatom gains relatively large energy and parallel momentum; assuming a hard-sphere collision with a collision diameter of 0.7 \AA on a flat surface, one can estimate for a typical $H(g)$ - $D_{ad}(H_{ad})$ collision at $b = 0.5 \text{ \AA}$ with an impact energy of $\sim 2.7 \text{ eV}$ (2.3 eV heat of adsorption plus 0.33 eV beam energy) an energy transfer of 1.2 eV (1.3 eV), of which the parallel energy of the s -HA accounts for 50%. A similar collision dynamics can be applied to the generation of s -HA's by the p -HA's most of which behave like the incident atoms. The normal energies of these s -HA's are much smaller than that of $H(g)$ and p -HA's and therefore they will experience a smaller corrugation than the latter atoms during their lateral hopping motions. Thus, we believe that a flat-surface model is not so unrealistic for the reactions of s -HA's, and hence the large desorption angles of the s -HA reaction products, D_2 as well as HD, peaked at $\sim 45^\circ$ are due to the large parallel momenta of s -HA's which are carried away

by the desorbing HD and D_2 product molecules. On a flat surface, internal excitations of the product molecules will further increase the desorption angle at the expense of the normal kinetic energy. The fraction of energy released as translation, vibration, and rotation measured for H-on- D_{ad} reaction on Cu(111) is that $f_t = 0.58$, $f_v = 0.26$, and $f_r = 0.16$ [7], indicating a high degree of internal excitations. Assuming the same value of $f_t = 0.58$, we calculate typical desorption angles of $\theta_f = 33^\circ$, 50° , and 42° for $H_s^* + D_{ad}$, $D_s^* + H_{ad}$, and $D_s^* + D_{ad}$ reactions, respectively. Despite the crude model and assumptions we made, the calculated typical desorption angles are more or less close to the observed peak angle of $\sim 45^\circ$. However, angle-resolved velocity and rovibrational distribution measurements are required to further elucidate the reaction dynamics. s -HA's which are less energetic than the reactive ones will also be generated, but most of them are expected to adsorb at empty sites left behind by the abstracted surface atoms to maintain the saturation coverage. In view of the small activation energy of $\sim 0.25 \text{ eV}$ [13] for the LH reaction, some of them may recombine with adsorbed $D(H)$ atoms in a similar way to ordinary thermal desorption resulting in a product angular distribution peaked at the surface normal, for example, a $\cos^{4.5} \theta_f$ distribution on Ni(111) [14]. The appreciable intensity (actually small if integrated over the desorption angle) of D_2 around $\theta_f \sim 0^\circ$ is probably due to such LH reactions.

This work has been supported in part by the Korean Science and Engineering Foundation through ASSRC at Yonsei University and by the KOSEF basic research project (97-05-010101-3).

*To whom all correspondence should be addressed.

Email address: jihwalee@plaza.snu.ac.kr

- [1] P.J. Eenshustra, J.H.M. Bonnie, J. Los, and H.J. Hopman, *Phys. Rev. Lett.* **60**, 341 (1988).
- [2] E.W. Kuipers, A. Vardi, A. Danon, and A. Amirav, *Phys. Rev. Lett.* **66**, 116 (1991).
- [3] B. Jackson and M. Persson, *J. Chem. Phys.* **96**, 2378 (1992).
- [4] C.T. Rettner, *Phys. Rev. Lett.* **69**, 383 (1992).
- [5] D.D. Koleske, S.M. Gates, and J.A. Schultz, *J. Chem. Phys.* **99**, 5619 (1993).
- [6] M. Persson and B. Jackson, *J. Chem. Phys.* **102**, 1078 (1995).
- [7] C.T. Rettner and D.J. Auerbach, *Phys. Rev. Lett.* **74**, 4551 (1995); *J. Chem. Phys.* **104**, 2732 (1996).
- [8] P. Kratzer, *J. Chem. Phys.* **106**, 6752 (1997).
- [9] S. Caratzoulas, B. Jackson, and M. Persson, *J. Chem. Phys.* **107**, 6420 (1997).
- [10] S.A. Buntin, *J. Chem. Phys.* **108**, 1601 (1998).
- [11] G. Eilmsteiner, W. Walkner, and A. Winkler, *Surf. Sci.* **352-354**, 263 (1996).
- [12] J.-Y. Kim and J. Lee (to be published).
- [13] K. Christmann and G. Ertl, *Surf. Sci.* **60**, 365 (1976).
- [14] H.P. Steinrück, K.D. Rendulic, and A. Winkler, *Surf. Sci.* **154**, 99 (1985).